

UDC 620; 544.472

<https://doi.org/10.33619/2414-2948/103/32>

DESIGN OF METAL SULFIDE ELECTRODE FOR HYDROGEN PRODUCTION BY ELECTROLYSIS

©Yang He, ORCID: 0009-0005-1559-2947, Jiangsu University of Science and Technology; Ogarev Mordovia State University, Zhenjiang, China; Saransk, Russia, 2206092043@qq.com

©Kudashev S., SPIN-код: 4763-0003, Ph.D., Ogarev Mordovia State University, Saransk, Russia, kudashev@mail.ru

ПРОЕКТИРОВАНИЕ МЕТАЛЛИЧЕСКОГО СУЛЬФИДНОГО ЭЛЕКТРОДА ДЛЯ ПОЛУЧЕНИЯ ВОДОРОДА ЭЛЕКТРОЛИЗОМ

©Ян Хэ, ORCID: 0009-0005-1559-2947, Цзянсуский университет науки и технологии, Национальный исследовательский Мордовский государственный университет им. Н.П. Огарева, г. Чжэньцзян, Китай; г. Саранск, Россия, 2206092043@qq.com

©Кудашев С. Ф., SPIN-код: 4763-0003, канд. техн. наук, Национальный исследовательский Мордовский государственный университет им. Н. П. Огарева, г. Саранск, Россия, kudashev@mail.ru

Abstract. Hydrogen evolution reaction (HER) is the cathodic hydrogen evolution reaction in electrolytic cell, but the hydrogen evolution catalytic properties of electrode materials best remains is the precious metal catalyst, therefore, in order to study the catalytic performance is good, and cheap hydrogen evolution electrode materials has become the research hot spot, metal sulfide can be mixed and with good electrical conductivity is it can be used as a necessary condition for hydrogen evolution electrode, The core theory of this paper is the first principle. By taking metal sulfide as the matrix and doping it with 10 metal group elements, Sc, Ti, V, Cr, Mn, Fe, Co, Ni, Cu and Zn, we obtained the configuration of 20 metal sulfide by doping it at two different sites of S atom, and inlaid H atom into metal atom. Then, through the use of software to study its catalytic performance, through the free energy analysis, rate analysis, bond length analysis, density of states analysis, charge analysis method, compared and found the most suitable doping metal element V, thus also determined that metal sulfide can be used as hydrogen evolution electrode through metal doping.

Аннотация. Реакция выделения водорода является катодной реакцией в электролитической ячейке, но каталитические свойства электродных материалов при выделении водорода лучше всего сохраняются при использовании драгоценных металлов, поэтому изучение каталитических характеристик является актуальным. Дешевые материалы с использованием сульфидов металлов с хорошей электропроводностью могут применяться для выделения водорода на электроде. Взяв сульфид металла в качестве матрицы и легировав его 10 элементами группы металлов, Sc, Ti, V, Cr, Mn, Fe, Co, Ni, Cu и Zn, мы получили конфигурацию 20 сульфидов металлов путем легирования их в двух различных местах атома S. Затем, с помощью программного обеспечения для изучения каталитических характеристик, с помощью анализа свободной энергии, анализа скорости, анализа длины связи, анализа плотности состояний, метода анализа заряда, сравнили и нашли наиболее подходящий легирующий элемент V. Таким образом было определено, что сульфид металла

может быть использован в качестве электрода для выделения водорода с помощью легирования металлом.

Keywords: metallic sulfide, cathode hydrogen evolution reaction, catalytic electrode for hydrogen evolution, hydrogen evolution performance analysis.

Ключевые слова: металлический сульфид, катодная реакция выделения водорода, каталитический электрод для выделения водорода, анализ эффективности выделения водорода.

Since fossil fuels remain the primary energy source worldwide, the environmental pollution resulting from their combustion, along with the issues of global warming and energy economic crises due to greenhouse gases, has garnered significant global attention. Hydrogen has the highest energy density among all chemical fuels, making it a prime candidate as the ultimate clean energy source for humanity. If it is to be regarded as the final energy carrier, hydrogen has the potential to substantially alleviate environmental problems stemming from the excessive carbon emissions associated with fossil fuels [1].

Many scientific researchers now often use electrolytic cell electrolysis of water to produce hydrogen. This method yields high-purity hydrogen, which can be used directly as raw material for industry or as household gas. Additionally, hydrogen is a highly efficient energy carrier that can be converted into various devices. Therefore, developing an efficient water electrolysis system for producing pollution-free hydrogen is essential.

The theory of water electrolysis is straightforward, with hydrogen and oxygen produced at the cathode and anode through the Hydrogen Extraction Reaction (HER) and Oxygen Extraction Reaction (OER), respectively. However, despite its simplicity, hydrogen production through water electrolysis has not been widely adopted on a large scale due to high costs associated with implementation in businesses or factories, expensive catalysts, and low efficiency with low-quality catalysts. As a result, the search for suitable catalysts continues. Currently, precious metal-based catalysts, particularly those based on Pt, play a decisive role in the electrochemical reaction. While Pt-based catalysts are among the most advanced and effective discovered by scientists, their high cost renders them unsuitable for large-scale use. Therefore, developing economical and highly active catalysts has become a top priority for water electrolysis systems. This paper focuses on investigating metal sulfides as electrodes for hydrogen production through electrolysis as part of the design process [2].

In Vija's research paper, the objective of his research is to investigate electrolyzer system modeling. This involves integrating various electrolytes into a mathematical framework that relies on foundational principles of thermal dynamics, electrochemistry, and system analysis [3]. Kristina Komander investigated the impact of absorbed hydrogen on the electronic energy deposition of 15N-ions in amorphous transition metal compounds, specifically vanadium (V) and zirconium (Zr), across varying concentrations [4]. Mir Sayed Shah Danish studied the classification, strategies, and potential applications of metal oxides in hydrogen evolution reaction (HER) catalysis. The study also discussed the green synthesis approach for applying these metal nanomaterials in energy storage and hydrogen production [5]. Ming Xiang utilized aromatic and aliphatic nitriles, which could be conveniently obtained, to achieve good yields and faradaic efficiencies when coupled with the hydrogen evolution reaction on the t-Ni/Co MOF electrode potential of 1.30 V vs [6]. Zafar Ali discovered that binary composites of transition metal sulfides (TMSs) exhibit superior electrochemical performance compared to both single sulfides and ternary sulfides [7]. In Lei Liu

research paper is synthesized by first creating CoMnLi hydroxide on the metal-organic framework Ni-BTC, followed by vulcanization through a solvent-thermal process. This electrode material exhibits a high specific capacity of 1040 C g⁻¹ at 1 A g⁻¹ and excellent cycling stability, retaining 87.94% capacity after 10,000 cycles utility [8]. In Lei Yang's research paper, hierarchical nanowires of MoS₂@transition metal sulfide (FeS, CuS, CoS₂, and SnS₂) heterostructures were fabricated using a simple process involving electrospinning, sulfuration, and subsequent hydrothermal treatment [9].

Currently, the primary method for preparing transition metal sulfides is chemical vapor deposition, which yields high-quality samples but has low overall efficiency, limiting its widespread use in electrochemical catalyst applications. In contrast, liquid-phase synthesis offers the advantage of large-scale production and is thus an important method for preparing transition metal sulfides in bulk. Experimental analysis suggests that various solvothermal methods for preparing metallic transition metal sulfide electrocatalysts have promising applications in actual water electrolysis for hydrogen production. Consequently, the development and application of metallic transition metal sulfides in electrochemistry have been effective. This paper aims to demonstrate the feasibility of using metal sulfides as electrodes for electrolytic hydrogen production. The participation of metal sulfides in hydrogen evolution reactions is primarily influenced by factors affecting the adsorption and desorption of hydrogen [10].

First Principles and Models

The first nature principle is derived from the Kohn-Sham (KS) equation, which is based on the non-relativistic framework of the Schrödinger equation for the molecular structure theory of single atoms. It provides a rigorous theoretical foundation, although the specific generalized function cannot be entirely free of relevant parameters. The calculation method begins with the atomic orbital system and involves continuous iterative calculations guided by the first nature principle. The goal is to reach a state where the energy error is minimized within a specified precision limit. This precision ensures that the calculated energy error is smaller than a predetermined threshold, indicating the completion of the calculation process.

Materials Studio is a software suite for materials analysis that can be run on PCs, supporting multiple operating platforms. It facilitates the creation of three-dimensional structural models and enables in-depth studies on the properties of various crystalline, amorphous, and polymeric materials, as well as related processes (Figure 1-3).



Figure 1. S placed in the top position of Ti

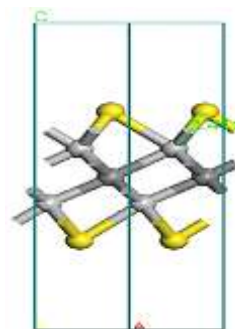
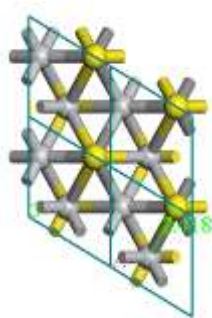


Figure 2. S placed in the hollow position of Ti

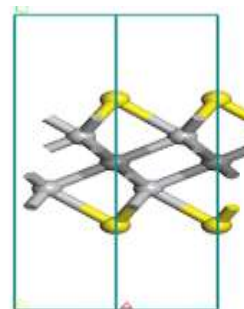
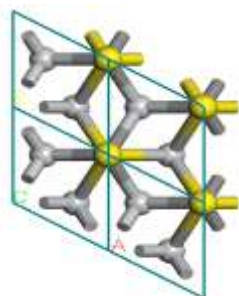


Figure 3. S placed in the top position of C

Among the three optimized models, the top site of Ti is considered to be the most preferred by comparing the energy, so the following operations are based on the top site of Ti. Click the S atom on the optimized matrix to copy and paste, select the copied S atom and click Modify Element button, and select the metal group element Sc in the periodic table to replace it. Place the S-atom in the top and hollow positions and bond it to the matrix to obtain two models, Sc1 and Sc2.

The performance of Sc1 and Sc2 is optimized, and we also optimize the precision in Medium for comparison. We found that the time difference between the optimization of Medium precision and Fine precision is particularly large, and Medium is relatively fast, which is because Fine precision has to be optimized in a more detailed way.

Repeat the above operation for Ti, V, Cr, Mn, Fe, Co, Ni, Cu, Zn nine metal group elements to carry out the same optimization optimization parameters remain unchanged. Create a hydrogen atom, adsorb the hydrogen atom onto a metal atom and follow the previous parameters, then optimize to get a model of a metal compound with 20 embedded hydrogen atoms. Create another hydrogen molecule model and optimize it for subsequent calculations. The free energy values are calculated from the Gibbs free formula below:

$$\Delta G = \Delta E + 0.24 \quad (1)$$

$$\Delta E = E_{\text{sys}} - E_{\text{cat}} - 1/2E_{\text{H}_2}$$

E_{sys} is the total energy of the metal compound after adsorption of hydrogen, E_{cat} is energy for the matrix, E_{H_2} is hydrogen energy.

Figure 4 below shows the Gibbs free energy distribution of metal atom doping sites at the top site of S. The order of free energy is Cu > Ni > Co > Fe > Mn > Cr > V > Sc > Zn > Ti, in which Zn has the smallest free energy of reaction, with a value of -1.15 eV, and Cu has the largest, with a value of 0.68 eV. The results of the existing studies show that the free energy of hydrogen is difficult to adsorb when it is higher than 0 eV, and the detachment of hydrogen is difficult when it is lower than 0 eV. free energy is high 0 eV, the adsorption of hydrogen atoms is difficult; when the

free energy is lower than 0 eV, the detachment of hydrogen is difficult. Therefore, when the free energy is close to 0 eV, the catalytic performance is optimal. According to the existing experimental basis, metal elements with free energies near plus or minus 0.3 eV can be candidates for catalysts. Here, we select a reasonable doping of transition metal elements based on the above activity criterion. It can be seen that the free energies of the doped configurations of six elements, Co, Cr, Fe, Mn, Cu, and Ni, are greater than 0 eV, i.e., there is a difficulty in hydrogen absorption, and the free energies of the doped configurations of four elements, Sc, Ti, V, and Zn, are less than 0 eV, i.e., there is a difficulty in dehydrogenation.

The free energies of the doped configurations of the elements Sc, Cr, V, Mn, and Fe are closest to 0 eV, with values of -0.04 eV, 0.08 eV, -0.03 eV, 0.16 eV, 0.25 eV, respectively, and thus have the best catalytic performance. Comparing the data of commercial Pt (whose free energy value is -0.09 eV), three metal elements such as Sc, Cr, and V have the best activity.

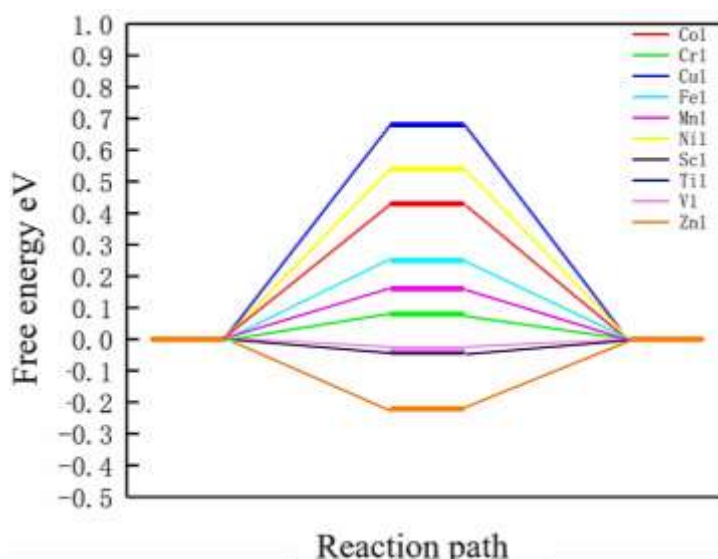


Figure 4. Reaction free energy of the top site

Analyzing the hollow position of metal atoms in the S atom, it can be seen from Figure 5 below that the free energy distribution is in the following order: $Cu > Ni > Co > Cr > Mn > V > Sc > Zn > Fe > Ti$, in which the maximum free energy of reaction of Cu is 0.64 eV, the minimum free energy of reaction of Ti is -1.31 eV, and with the figure, it can be seen that the free energy of reaction of Cu, Ni, Cr, Co, Mn is greater than 0 eV, i.e., there are difficulties in hydrogen precipitation, V, Sc, Zn, Fe, Ti is less than 0 eV, and there are difficulties in dehydrogenation.

The free energy of reaction of Cu, Ni, Cr, Co, Mn is greater than 0 eV, i.e., there is a difficulty in hydrogen precipitation, and the free energy of reaction of V, Sc, Zn, Fe, Ti is less than 0 eV, i.e., there is a difficulty in dehydrogenation, and among them, the free energies of reaction of the doped configurations of Sc, Cr, V, and Mn are the closest to 0 eV, with values of -0.08 eV, 0.07 eV, -0.05 eV, and 0.06 eV, respectively, and therefore they have the best catalytic performances. Comparing the data of commercial Pt (whose free energy value is -0.09 eV), four metal elements such as Sc, Cr, V, and Mn have the best activity.

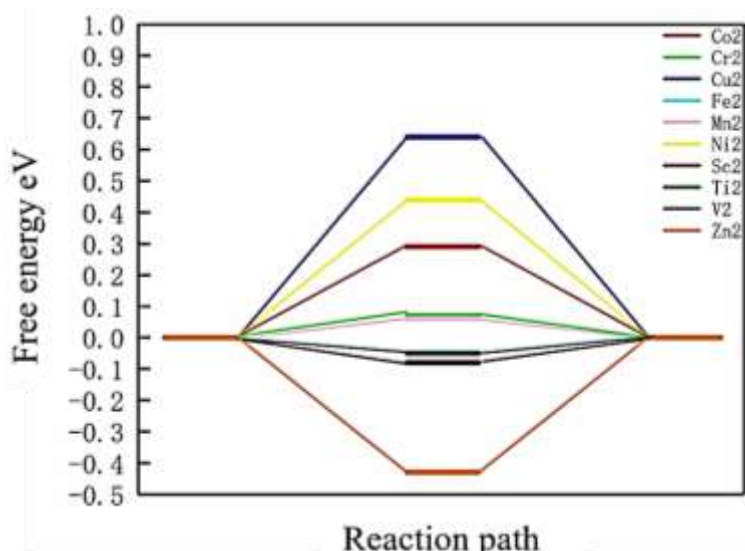


Figure 5. Reaction free energy of the hollow site

We analyzed the comparison between different metals at top position and hollow above, and took the data of commercial Pt (whose free energy value is -0.09 eV) as the base, and selected three elements Sc, Cr, V at top position, and Sc, Cr, V, Mn at hollow, because the value of Mn's top position doesn't meet the requirement, but its hollow is in accordance with the requirements, can be used to analyze and compare, so we will Sc, Cr, V, Mn, the four metals are selected, their different positions of the free energy size of the comparison between the following Figure 6 shows, the figure after the metal number, 1 represents the top position, 2 represents the hollow position.

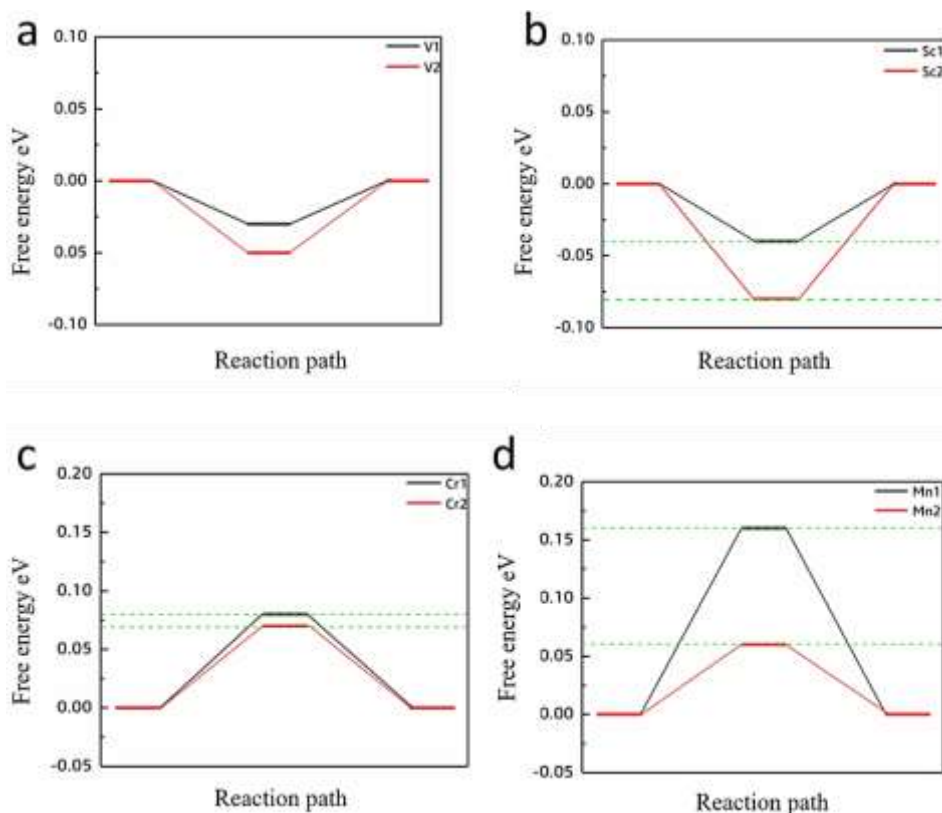


Figure 6. Comparison of free energy at different positions (a: free energy at different positions of V, b: free energy at different positions of Sc, c: free energy at different positions of Cr, d: free energy at different positions of Mn)

In Figure a, the free energy of V in top position is -0.03 eV, and the free energy in hollow position is -0.05 eV, so the energy curves of V in top position and hollow position are actually very close to each other, and we can see that the hollow position of V is below the energy of top position in the figure, which is that the energy required for hydrogen detachment in the process of hydrogen detachment when V is located in the hollow position is a little bit more. This is because it takes more energy for hydrogen to detach when V is in the hollow position. This is because it takes more energy to detach hydrogen from V in the hollow position. If the hydrogen is not detached in time, hydrogen poisoning will occur, so the top position of V is better than the hollow position.

In Fig. b, we can see that similar to Figure a, Sc's hollow position is below the energy of the top position but the free energy of Sc in the top position is -0.04eV, and the free energy in the hollow is -0.08eV, so the same as the law of V above, the top position of Sc is superior to the hollow, and the free energy of the two positions is greater than the V in the comparison, so the catalytic efficiency of V is greater than that of Sc. In Fig. c, we can see that the free energy of Cr is greater than 0 in both positions, and the hollow position is below the energy of the top position, the free energy of Cr is 0.08eV in the top position, and the free energy of Cr is 0.07eV in the hollow position, which is different from the principle above, the higher the energy when the free energy is greater than 0 means that the energy required in the hydrogen adsorption will be higher, therefore, Cr is worse than the hollow in the top position. Therefore, the top position of Cr is worse than the hollow position, because it takes more energy to make hydrogen adsorption. In Fig. d, we can see that the free energy of Mn in top position is 0.16 eV, and that of Mn in hollow position is 0.06 eV, because the values of free energy are greater than 0. Therefore, the same law as that of Cr above, the free energy of Mn in hollow position is smaller than that of top position, and so the free energy of Mn in top position is also worse than that in hollow position.

Therefore, we statistically show that the best catalytic performance is the embedded V metal sulfide, no matter the top site or the hollow site. The worst catalytic performance is the embedded Ti metal sulfide.

We got the conclusion in the previous section that the best catalytic performance is embedded V-metal sulfides and the worst catalytic performance is embedded Ti-metal sulfides, we in order to determine the main influences on the catalytic performance, we first carry out the rate analysis, we need to use the formula of Arrhenius formula, the formula is as follows:

$$k = Ae^{-Ea/RT} \quad (2)$$

k denotes the rate we want to get, A is a constant called the pre-factor, Ea we use the free energy ΔG from above, R is the molar gas constant we take the approximate value 8.314 in our calculations, T is the thermodynamic temperature.

Because the metal compound catalysts we used in the course of our experiments produce compounds with S at both top and hollow sites during the reaction, the free energy of Pt metal is known to be -0.09 eV according to the data, so we chose to use the metal compounds as catalysts in order to be able to find a replacement for the Pt metal catalysts to compare the hydrogen precipitation rate with the Pt metal catalysts and chose the best catalytic performance of V metal sulfide and the worst catalytic performance of Ti metal sulfide after inlaying. The best catalytic performance of V metal sulfide and the worst catalytic performance of Ti metal sulfide after inlaying were used for the calculation using the Arrhenius formula above, where A is a constant that does not affect the relative magnitude of the calculation results and need not be involved in the calculation process. The results of calculating the catalytic rate are shown in Table below. In the Table below the numbers 1 and 2 indicate that the metal atoms are located at the top and hollow sites of S, respectively, and the metal atoms represent the rate constants.

Table

RATE CONSTANTS AT DIFFERENT TEMPERATURES

$T(K)$	Pt	$V1$	$V2$	$Ti1$	$Ti2$
300	0.9633	0.9876	0.9794	0.6201	0.5802
400	0.9723	0.9907	0.9845	0.6988	0.6648
500	0.9778	0.9925	0.9876	0.7507	0.7214
600	0.9815	0.9938	0.9897	0.7875	0.7617
700	0.9841	0.9947	0.9911	0.8148	0.7919
800	0.9861	0.9953	0.9922	0.8359	0.8154

In the above table, because our normal reaction process are at room temperature 300 K as can clearly see the rate constant with the increase in temperature and increasing, in which we choose a better embedded V metal sulfide no matter in the top position or hollow position of the rate is greater than the reaction rate of Pt metal catalysts and embedded Ti metal sulfide in both positions than the Pt metal catalysts of the reaction rate is small, so we initially judged that we can choose embedded V metal sulfide as a replacement for the Pt metal catalysts catalyst materials.

Through the above analysis of the catalytic performance factors, we found that the bond length and charge of metal atoms are not the main factors affecting their catalytic performance, so we next carry out the density of states analysis, the density of states is the result of the visualization of the energy band structure as we know it, and we can use the Materials studio software to carry out the energy band analysis of the metal atoms and the hydrogen atoms that we selected, so that we can get the different distributions of electrons in the s orbitals and d orbitals. In the charge analysis above, we have selected the embedded Ti metal sulfide with the worst catalytic performance and the embedded V metal sulfide with the best catalytic performance, in which the free energy of Ti in the top position is -1.15 eV, and that in the hollow position is -1.31 eV. There is a big difference in the free energies of the two positions, and in order to investigate the reason for this difference, we use the software's In order to study the reason for this difference, we used the analysis function of the software to analyze the energy bands of Ti atoms and hydrogen atoms embedded in the top and hollow sites, and the orbital analysis diagrams are shown in Figure 7 below.

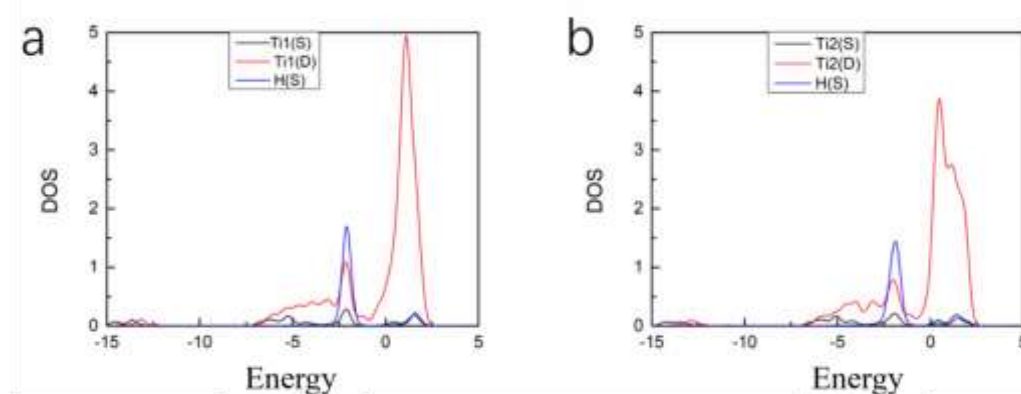


Figure 7. Density state analysis of Ti (a: Ti embedded in top site, b: Ti embedded in hollow site)

In the figure, in order to show clearly, we will be located in the top position of the Ti atom labeled as Ti1, will be located in the hollow of the Ti atom labeled as Ti2, the left axis is the density of states, the lower axis is the energy. We look at the upper right scale of the figure shows that the black curve is the s-orbital curve of Ti, the red curve is the d-orbital curve of Ti, and the blue curve is the s-orbital curve of H. Next, we first analyze the a-figure, in which the highest peak of the blue curve (the s-orbital of H) corresponds to the peak of the second peak of the red curve (Ti),

indicating that the magnitude of the free energy of the Ti atom located in the top position is controlled by these two peaks. We localize the two peaks, and the energy coordinate corresponding to the peak of the blue curve (s orbital of H) is at -2.08 eV, and the energy coordinate corresponding to the peak of the red curve (Ti) is at -2.16 eV. We now look at the b plot, which has the same labeling of the curves except that the Ti atom is labeled Ti2 when it is located in the hollow, and the blue curve (s orbital of H) has the same labeling of the curves. The highest peak of the blue curve (s orbital of H) corresponds to the peak of the third peak of the red curve (Ti), again indicating that the magnitude of the free energy of Ti when it is in the hollow position is controlled by these two peaks. We also localize the peaks of the blue curve (S orbital of H) at -1.89 eV and the peak of the red curve (Ti) at -2.03 eV, and compare the two sets of energy coordinates, and find that the energy coordinates of Ti metal embedded in the top position of S are larger than that of the top position of S, which is closer to the Fermi energy level bounded by 0 eV. We hypothesize that this is the reason why the free energy of the top site is better than that of the hollow site. In order to prove our current speculation, we perform the above operation on the V atom, which has good catalytic performance in both sites above, and whose free energy is -0.03 eV in the top site and -0.05 eV in the hollow site, and the orbital analysis diagrams of V in the top site and the hollow site are shown in Figure 8 below.

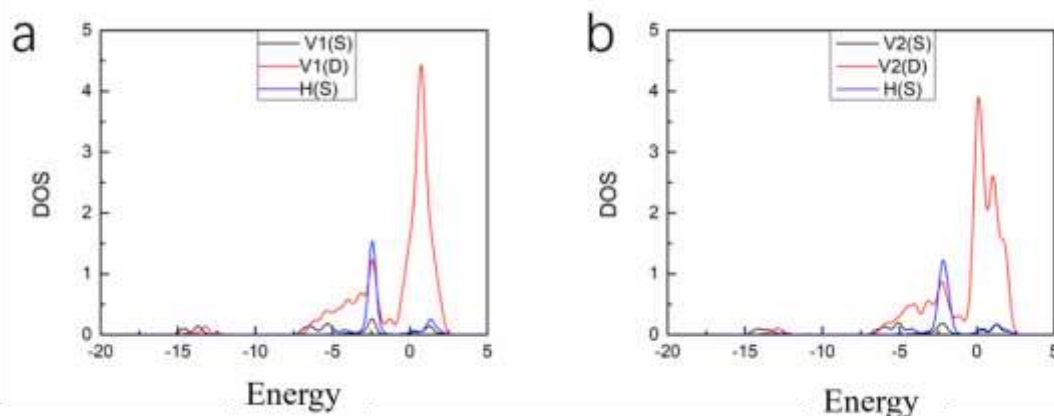


Figure 8. Density state analysis of V (a:V embedded in top site, b:V embedded in hollow site)

We repeat the above operation, in which we only need to change the name of the metal atom from Ti to V. We first analyze the a diagram, observing the curves, we find that the highest peak of the blue curve (s-orbital of H) corresponds to the peak of the second peak of the red curve (V) and the same as in the above result is that the highest peak of H is larger than the second peak of V. We also locate the energy coordinates of the blue curve (s-orbital of H) and the energy coordinates of the red curve (V).

The energy coordinates of the blue curve (s-orbit of H) and the red curve (V) are localized, and the energy coordinates of the blue curve (s-orbit of H) are -2.45 eV, and the energy coordinates of the red curve (V) are -2.39 eV, and the energy coordinates of V are -2.39 eV, and the energy coordinates of V are -2.45 eV, and the energy coordinates of V are -2.45 eV, and the energy coordinates of V are -2.39 eV, and the energy coordinates of V are -2.39 eV.

The energy coordinates of the blue curve (s-orbital of H) are -2.18 eV, and the energy coordinate of the red curve (V) is -2.28 eV. We find that the peak value of V and the peak value of H correspond to the value of Ti, which is smaller, and we can think that the smaller the value of the energy coordinate is, i.e., the farther away from the Fermi level, the closer the absolute value of the

free energy is to 0 eV, and the better the catalytic performance is, so the magnitude of free energy is related to the metal atoms, and the catalytic performance is better. Therefore, the size of the free energy is related to the density of states of metal and hydrogen atoms.

By analyzing and comparing the adsorption capacity of adsorbing a single hydrogen atom when metal atoms are located at different positions in metal sulfides, it is found that the free energies of metal atoms located at the top position and at the hollow position of S and the free energies of different metal doping are different, and that the adsorption capacity can be adjusted by doping with different metals and by controlling the doping is the position of metal atoms. When a hydrogen atom is adsorbed, the magnitude of free energy is in the order of $\text{Cu} > \text{Ni} > \text{Co} > \text{Fe} > \text{Mn} > \text{Cr} > \text{V} > \text{Sc} > \text{Zn} > \text{Ti}$ for the top site of S, and in the order of $\text{Cu} > \text{Ni} > \text{Co} > \text{Cr} > \text{Mn} > \text{V} > \text{Sc} > \text{Zn} > \text{Fe} > \text{Ti}$ for the hollow site of S. Then we find that the free energies of different metal doped at the top site of S and different metal doped at the hollow site of S are different. The free energy of a metal in the top site of S is larger than that of a metal in the hollow site of S.

Mechanistic analysis of the configurations revealed that the rate of metal sulfides with embedded V was found to be higher than the catalytic rate of the Pt catalyst by rate analysis of the configurations, and the rate increased with increasing temperature. After that, bond length analysis was performed on the conformations and we analyzed the fitted curves of bond length and free energy and found that there is no linear relationship between bond length and free energy, which may be due to the coexistence of ionic and covalent bonds. We then performed charge analysis on the conformations and obtained the conclusion that the effect of electrostatic force on the adsorption energy is not absolute by using the embedded V-metal sulfide, which has the best hydrogen-dissolving catalytic performance, and the embedded Ti-metal sulfide, which has the poorer hydrogen-dissolving catalytic performance, for comparison. The density of states analysis of the configuration was carried out, and the result obtained is that we can consider that the smaller the value of the energy coordinate is, the closer the absolute value of the free energy is to 0. Therefore, the magnitude of the free energy is related to the density of states of the metal atoms and hydrogen atoms. The feasibility of metal sulfides as hydrogen precipitation electrodes was confirmed, especially the embedded V metal sulfides, which have superior catalytic properties and stability.

References:

1. Bello, M. O., & Ch'ng, K. S. (2024). Path to clean and sustainable energy from nuclear and renewable sources: Evidence from France. *Utilities Policy*, 88, 101764. <https://doi.org/10.1016/j.jup.2024.101764>
2. Liu, Z., Deng, Y., Wang, P., Wang, B., Sun, D., & Yu, B. (2024). Study on the gas-liquid two-phase flow patterns for hydrogen production from electrolytic water. *International Journal of Hydrogen Energy*, 60, 711-728. <https://doi.org/10.1016/j.ijhydene.2024.02.102>
3. Kumar, V., & Tiwari, A. K. (2024). Performance assessment of green hydrogen generation via distinct electrolytes dedicated to renewable energy. *Desalination*, 582, 117651. <https://doi.org/10.1016/j.desal.2024.117651>
4. Komander, K., Malinovskis, P., Pálsson, G. K., Wolff, M., & Primetzhofer, D. (2024). Accurate measurement of hydrogen concentration in transition metal hydrides utilizing electronic excitations by MeV ions. *International Journal of Hydrogen Energy*, 57, 583-588. <https://doi.org/10.1016/j.ijhydene.2024.01.032>
5. Danish, M. S. S. (2023). Exploring metal oxides for the hydrogen evolution reaction (HER) in the field of nanotechnology. *RSC Sustainability*, 1(9), 2180-2196. <https://doi.org/10.1039/D3SU00179B>

6. Xiang, M., Xu, Z., Wu, Q., Wang, Y., & Yan, Z. (2022). Selective electrooxidation of primary amines over a Ni/Co metal-organic framework derived electrode enabling effective hydrogen production in the membrane-free electrolyzer. *Journal of Power Sources*, 535, 231461. <https://doi.org/10.1016/j.jpowsour.2022.231461>
7. Ali, Z., Iqbal, M. Z., & Hegazy, H. H. (2023). Recent advancements in redox-active transition metal sulfides as battery-grade electrode materials for hybrid supercapacitors. *Journal of Energy Storage*, 73, 108857. <https://doi.org/10.1016/j.est.2023.108857>
8. Liu, L., Li, H., Jiang, S., Zhao, Q., & Jiang, T. (2024). Design of high-performance transition metal sulfide electrode materials and its application in supercapacitors. *Journal of Power Sources*, 606, 234560. <https://doi.org/10.1016/j.jpowsour.2024.234560>
9. Yang, L., Yuan, X., Dong, Y., Qian, S., & Zhu, C. (2024). Hierarchical nanowires of MoS₂@ transition metal sulfide heterostructures for efficient electrocatalytic hydrogen evolution reaction. *Journal of Electroanalytical Chemistry*, 118342. <https://doi.org/10.1016/j.jelechem.2024.118342>
10. Tong, Y., Hou, Y., Zhang, Z., Yan, L., Chen, X., Zhang, H., ... & Li, Y. (2023). Current progress of metal sulfides derived from MOFs for photocatalytic hydrogen evolution. *Applied Catalysis A: General*, 119387. <https://doi.org/10.1016/j.apcata.2023.119387>

Список литературы:

1. Bello M. O., Ch'ng K. S. Path to clean and sustainable energy from nuclear and renewable sources: Evidence from France // *Utilities Policy*. 2024. V. 88. P. 101764. <https://doi.org/10.1016/j.jup.2024.101764>
2. Liu Z., Deng Y., Wang P., Wang B., Sun D., Yu B. Study on the gas-liquid two-phase flow patterns for hydrogen production from electrolytic water // *International Journal of Hydrogen Energy*. 2024. V. 60. P. 711-728. <https://doi.org/10.1016/j.ijhydene.2024.02.102>
3. Kumar V., Tiwari A. K. Performance assessment of green hydrogen generation via distinct electrolytes dedicated to renewable energy // *Desalination*. 2024. V. 582. P. 117651. <https://doi.org/10.1016/j.desal.2024.117651>
4. Komander K., Malinovskis P., Pálsson G. K., Wolff M., Primetzhofer D. Accurate measurement of hydrogen concentration in transition metal hydrides utilizing electronic excitations by MeV ions // *International Journal of Hydrogen Energy*. 2024. V. 57. P. 583-588. <https://doi.org/10.1016/j.ijhydene.2024.01.032>
5. Danish M. S. S. Exploring metal oxides for the hydrogen evolution reaction (HER) in the field of nanotechnology // *RSC Sustainability*. 2023. V. 1. №9. P. 2180-2196. <https://doi.org/10.1039/D3SU00179B>
6. Xiang M., Xu Z., Wu Q., Wang Y., Yan Z. Selective electrooxidation of primary amines over a Ni/Co metal-organic framework derived electrode enabling effective hydrogen production in the membrane-free electrolyzer // *Journal of Power Sources*. 2022. V. 535. P. 231461. <https://doi.org/10.1016/j.jpowsour.2022.231461>
7. Ali Z., Iqbal M. Z., Hegazy H. H. Recent advancements in redox-active transition metal sulfides as battery-grade electrode materials for hybrid supercapacitors // *Journal of Energy Storage*. 2023. V. 73. P. 108857. <https://doi.org/10.1016/j.est.2023.108857>
8. Liu L., Li H., Jiang S., Zhao Q., Jiang T. Design of high-performance transition metal sulfide electrode materials and its application in supercapacitors // *Journal of Power Sources*. 2024. V. 606. P. 234560. <https://doi.org/10.1016/j.jpowsour.2024.234560>

9. Yang L., Yuan X., Dong Y., Qian S., Zhu C. Hierarchical nanowires of MoS₂@ transition metal sulfide heterostructures for efficient electrocatalytic hydrogen evolution reaction // Journal of Electroanalytical Chemistry. 2024. P. 118342. <https://doi.org/10.1016/j.jelechem.2024.118342>
10. Tong Y., Hou Y., Zhang Z., Yan L., Chen X., Zhang H., Li Y. Current progress of metal sulfides derived from MOFs for photocatalytic hydrogen evolution // Applied Catalysis A: General. 2023. P. 119387. <https://doi.org/10.1016/j.apcata.2023.119387>

*Работа поступила
в редакцию 18.05.2024 г.*

*Принята к публикации
24.05.2024 г.*

Ссылка для цитирования:

Yang He, Kudashev S. Design of Metal Sulfide Electrode for Hydrogen Production by Electrolysis // Бюллетень науки и практики. 2024. Т. 10. №6. С. 284-295. <https://doi.org/10.33619/2414-2948/103/32>

Cite as (APA):

Yang, He, & Kudashev, S. (2024). Design of Metal Sulfide Electrode for Hydrogen Production by Electrolysis. *Bulletin of Science and Practice*, 10(6), 284-295. <https://doi.org/10.33619/2414-2948/103/32>